Simulation of the soft-landing and adsorption of C_{60} molecules on a graphite substrate and computation of their scanning-tunnelling-microscopy-like images

2000 J. Phys.: Condens. Matter 12 5551

(http://iopscience.iop.org/0953-8984/12/26/303)

J. Phys.: Condens. Matter **12** (2000) 5551–5563. Printed in the UK PII: S0953-8984(00)11907-1

Simulation of the soft-landing and adsorption of C_{60} molecules on a graphite substrate and computation of their scanning-tunnelling-microscopy-like images

H Rafii-Tabar†, L Jurczyszyn‡ and B Stankiewicz‡

† Computational Nano-Science Research Group, Centre for Numerical Modelling and Process Analysis, School of Computing and Mathematical Sciences, University of Greenwich, Greenwich Maritime Campus, 30 Park Road, Greenwich, London SE10 9LS, UK
‡ Institute of Experimental Physics, University of Wroclaw, Pl. M Borna 50-204, Wroclaw, Poland

Received 16 February 2000, in final form 28 April 2000

Abstract. A constant-temperature molecular dynamics (MD) simulation was performed to model the soft-landing and adsorption of C_{60} molecules on a graphite substrate with the C_{60}s treated as soft molecules and released individually towards the substrate. The intra-molecular and intra-planar covalently bonding interactions were modelled by very accurate many-body potentials, and the non-bonding forces were derived from various pairwise potentials. The simulation extended over 1.6 million time steps covering a significant period of 160 picoseconds. The final alignment of the molecules on the surface agrees closely with that observed in an experiment based on scanning tunnelling microscopy (STM) on the same system, performed at room temperature and under ultrahigh-vacuum (UHV) conditions. Using a tungsten tip in a constant-current mode of imaging, we have also computed the STM-like images of one of the adsorbed molecules using a formulation of the STM tunnelling current based on Keldysh's non-equilibrium Green function formalism. Our aim has been to search for tip-induced states, which were speculated, on the basis of another STM-based experiment, performed in air, to form one of the possible origins of the extra features purported to have been observed in that experiment. We have not obtained any such states.

1. Introduction

The exploitation of the unique properties of the fullerenes, and in particular of C_{60}, in nanoscopic device fabrication and processes, such as nanolithography [1, 2], requires the adsorption of these molecules on a variety of supporting substrates. This has prompted research, using STM and other techniques, into the early stages of nucleation and growth of fullerene monolayer and multilayer films on metallic, semi-metallic, semiconducting and oxide surfaces. Information on the growth mode and morphology of the first few layers will help determine the characteristics of the resulting films. Aspects of this research involving the adsorption on the Si(100) 2×1, the Si(111) 7×7, the Cu(111) 1×1 and the Ag(111) surfaces have been reviewed [3], and it can be seen that in general on metallic substrates the observed monolayers form close-packed quasi-hexagonal alignments similar to the (111) plane of the fcc C_{60} crystal [4–8], while on semiconducting surfaces the C_{60}s form disordered films that are, however, locally ordered [9–13]. It is also known that the C_{60} layer grown on the Au(111) surface [14, 15] is structurally unstable and forms *mobile* hexagonal arrays of sub-clusters with a spacing of 11.0 Å, and the layer grown on the GaAs(110) surface [16, 17]

0953-8984/00/265551+13$30.00

shows locally ordered large monolayer islands that are structurally stable and commensurate with the substrate.

The study of the formation of a C_{60} film on graphite is of interest since there is a strong similarity in the electronic and geometrical structures of these two materials. Several experimental, as well as theoretical, investigations of this system have been reported so far. A high-resolution electron energy-loss spectroscopy (HREELS) experiment [18], performed under UHV conditions, on the structural and vibrational properties of the C_{60} film adsorbed on the surface of highly oriented pyrolytic graphite (HOPG) showed a novel high-order periodicity at monolayer coverages, implying that even the weak corrugation potential of the surface was sufficient to perturb the adlayer, and that the C_{60}s were *physisorbed* on the graphite. Another HREELS-based experiment [19] on the early stages in growth at room temperature has suggested a predominantly layer-by-layer growth of two-dimensional islands, while a combined HREELS-and-STM-based experiment [20, 21] on the adsorption of C_{60} molecules on a HOPG (0001) surface, performed under UHV conditions at room temperature, showed that the adsorbed molecules aggregated to form asymmetric dendrite-like islands, implying a high mobility on the surface. Higher magnification of the STM images in this experiment also revealed that the C_{60}s arranged themselves in a hexagonal close-packed morphology, and two crystallographic directions were identified. Furthermore, this experiment also showed that the growth mode on the surface was consistent with both the Frank–van der Merwe layer-by-layer mode and the mixed monolayer-plus-island Stranski–Krastanov mode. Very recently, the results of another STM-based experiment [22], performed under UHV conditions and at substrate temperatures of 300 K and 373 K, carried out to examine the role of the deposition rate and the temperature, and the influence of naturally occurring HOPG surface steps on the growth of C_{60} islands have been reported. It was found that at room temperature, multilayer islands of C_{60}, of different sizes, were nucleated predominantly at the step edges, with a negligible formation on the terraces. Unlike in other studies, a simple layer-by-layer growth mode was only observed at the elevated temperature. Furthermore, the basis of a three-dimensional growth was found to be an initial bilayer, rather than a monolayer, formation. The lowering of the deposition rate promoted the formation of islands with faceted edges, indicating that at a lower rate the molecules arriving at an island edge had sufficient time to diffuse around the island and take up a more ordered equilibrium structure.

In addition to these UHV-based STM experiments, another STM-based experiment performed in air, where C_{60} molecules were adsorbed from a solution onto HOPG [23], showed C_{60} molecules forming clusters of various sizes that had a tendency to aggregate further. Furthermore, detailed examination of the STM images had shown what were claimed to be extra features, in the form of *ridges* and *bumps*, on individual molecules. It was suggested that these could represent real structures, but their origins could not be unambiguously identified and they were attributed to electronic states induced either by the action of the HOPG substrate or by the STM tip on the charge states of the C_{60} molecules.

The C_{60}–graphite system has also been investigated theoretically. Ruoff and Hickman [24] developed a potential for the interaction of a C_{60} molecule, modelled as a hollow sphere with the carbon atoms uniformly distributed on its surface with a specified density, and a graphite plane, modelled as a continuum sheet. The sphere–plane potential was obtained by assuming a Lennard-Jones (12–6) atom–atom potential integrated over all the atoms. The potential was used to determine the force constants and vibrational frequencies of the sphere–plane system as well as the Arrhenius expression for the desorption of the sphere from the surface. The Ruoff–Hickman C_{60}–graphite potential was used by Rey *et al* [25] to obtain the most stable configurations of C_{60} molecules supported by a graphite substrate. The molecules, modelled as hollow spheres, were supported by the substrate, modelled as a continuum sheet, from the start,

i.e. not dynamically deposited during an adsorption process. The equilibrium configurations, corresponding to the minima in the potential energy surface, were then searched for via a MD simulation starting with an arbitrary initial configuration of the C_{60}s. It was predicted that the ground-state structures of the supported molecules consisted of monolayer-like hexagonal arrangements parallel to the graphite surface with the most stable structures occurring for clusters containing 7, 19, 37 and 61 C_{60}s. The equilibrium gap between the centres of mass of the C_{60} molecules in the first layer and the graphite sheet was found to be 6.5295 Å. In another theoretical study, Gravil *et al* [26] calculated the van der Waals energy of a C_{60} molecule adsorbed on a graphite-like substrate and on the $C_{60}(111)$ surface and found that the adsorption energies on these surfaces were respectively 968 meV and 813 meV, and the diffusion barrier at room temperature over graphite was only 13 meV, smaller than kT, and much smaller than that over the $C_{60}(111)$ surface (168 meV), indicating a relatively high mobility of the C_{60} over the graphite surface. Furthermore, it was found that the equilibrium gap between the centre of the molecule and the graphite-like surface was 6.55 Å, very close to the result of Rey *et al* [25].

In this paper we first study the C_{60}–graphite system within the framework of a *dynamic* adsorption process under conditions that are fairly similar to those of a typical STM-based deposition experiment performed under UHV conditions, such as [21]. For this purpose, we perform a constant-temperature MD simulation to model the complete process of the soft-landing and adsorption of several C_{60} molecules on the (0001) basal plane of a graphite substrate. Next, we examine the claims made by Yu *et al* [23] on the observation of extra features on C_{60} molecules. For this, we calculate the STM-like images of one of the adsorbed molecules, extracted from the final-state *equilibrium* alignment obtained in the MD simulation. We specifically investigate the validity of their suggestion that tip-induced states could be one possible mechanism for giving rise to these features.

2. The MD simulation

2.1. Inter-atomic potentials

The energetics and dynamics of the C_{60}–graphite system were obtained from four different inter-atomic potentials. Here we state their general functional forms. The detailed description of their terms and the corresponding potential parameters are given in [27].

2.1.1. The carbon–carbon non-bonding potentials. The relatively weak non-bonding interactions between the carbon atoms in two C_{60} molecules and in two graphite basal planes were respectively described by the 6-exp [28] and the Lennard-Jones [29] potentials

$$H_I^{DJ}(r_{ij}^{IJ}) = \sum_i \sum_{j>i} -\frac{A}{(r_{ij}^{IJ})^6} + B\mathrm{e}^{-\alpha r_{ij}^{IJ}} \tag{1}$$

and

$$H_I^{LJ}(r_{ij}^{IJ}) = 4\epsilon \sum_i \sum_{j>i} \left[\left(\frac{\sigma}{r_{ij}^{IJ}} \right)^{12} - \left(\frac{\sigma}{r_{ij}^{IJ}} \right)^{6} \right] \tag{2}$$

where I and J denote the two molecules (planes); r_{ij}^{IJ} is the distance between the atom i in molecule (plane) I and the atom j in molecule (plane) J.

2.1.2. The non-bonding C_{60}–graphite potential. The C_{60}–graphite interfacial interactions were described by the Ruoff–Hickman potential [24]. However, only the C_{60}s were modelled as continuum hollow spheres (radius $b = 3.55$ Å) during these interactions and the graphite

substrate was treated as a lattice of individual atoms. Under this approximation the Ruoff–Hickman potential, now describing the interaction of a hollow sphere with a single atom of the graphite substrate, takes on the form

$$V(z) = V_{12}(z) - V_6(z) \tag{3}$$

where

$$V_n(z) = \frac{c_n}{2(n-2)}\frac{N}{bz}\left[\frac{1}{(z-b)^{n-2}} - \frac{1}{(z+b)^{n-2}}\right] \tag{4}$$

with N being the number of atoms on the sphere ($N = 60$ in this case), $n = 12, 6$ and $z > b$ is the distance of the graphite atom from the centre of mass of the sphere.

2.1.3. The covalently bonding carbon–carbon potentials. The intra-molecular and intra-planar interactions were described by the powerful and improved many-body Tersoff-type Brenner potentials [30–32]

$$H_I^{Br} = \frac{1}{2}\sum_i \sum_{i \neq j} V(r_{ij}) \tag{5}$$

where

$$V(r_{ij}) = f_c(r_{ij})\left[V^R(r_{ij}) + \bar{b_{ij}} V^A(r_{ij})\right]. \tag{6}$$

These potentials are parametrized in terms of a very large database of numerical data on parameters and spline functions.

2.2. Simulation of the soft-landing and adsorption process

The initial state, shown in figure 1(a), consisted of 14 *flexible* C_{60} molecules randomly distributed above the (0001) basal plane of a graphite substrate composed of three planes with respectively 448, 448 and 568 atoms in the upper, middle and lower planes. The substrate was constructed with this configuration so as to allow for the presence of both terraces and steps in the case of terrace diffusion leading to the segregation of the molecules at the steps. The simulation time step and temperature were set respectively at $dt = 10^{-16}$ s and $T = 300$ K, and the velocity Verlet algorithm [33] was used to integrate the equations of motion. The simulation temperature was maintained at this value by implementing a Nosé–Hoover thermostat [34, 35] for realizing a canonical ensemble. An equilibration phase of 10 000 time steps, during which the C_{60}s were not allowed to move in the z-direction, or interact with each other or with the substrate, was first performed. All other interactions, i.e. the intra-molecular, intra-planar and inter-planar interactions, were, however, switched on. We observed an insignificant strain of about 0.025% in the total volume of the system during this phase, and a shift of the graphite basal planes relative to their initial states, as shown in figure 1(b).

Following equilibration, the molecules were *individually* released towards the substrate, one at a time, with a kinetic energy corresponding to the constant temperature of $T = 300$ K. This deposition technique ensured that there were no correlations between the molecules prior to their soft-landing and adsorption on the graphite surface. The dynamical adsorption method that we followed consisted of the following steps. First a molecule was released from its equilibrated position. Its history was then followed until it soft-landed on the substrate and equilibrated with it after undergoing several bounce-on–bounce-off vertical motions, as well as lateral diffusive motions, over the surface. Once the molecule was adsorbed, the next one was then released. When monitoring the state of a newly released molecule, the dynamics of the molecules already adsorbed were also followed simultaneously, i.e. when a new molecule

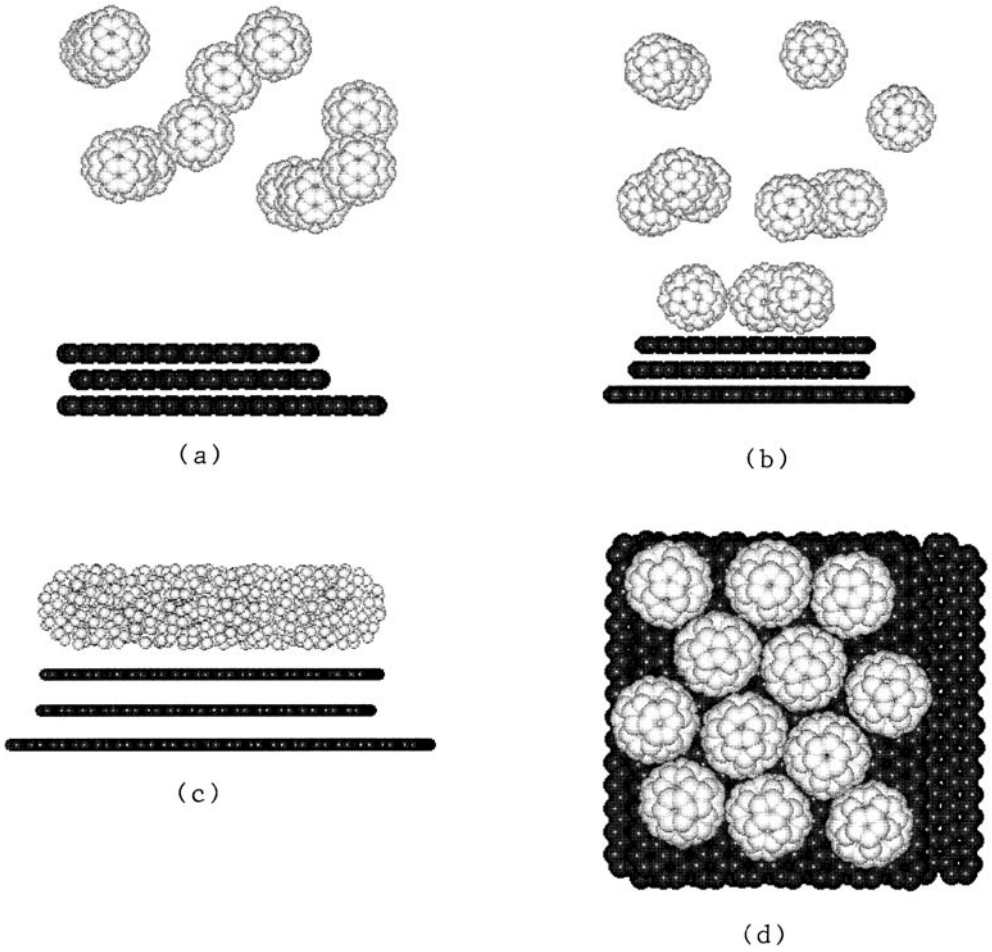

Figure 1. Three-dimensional snapshots from the MD simulation showing the C_{60}–graphite system: in the initial state (a); after 22 picoseconds (b); after 161 picoseconds (c); and the top view after 161 picoseconds (d). The ⟨100⟩ direction runs from left to right.

was heading towards the substrate the interactions among those molecules already adsorbed, and between them and the substrate, were also considered at the same time. When a new molecule was adsorbed, the overall system was re-equilibrated before another molecule was released. The C_{60}–C_{60} interactions were switched on only for those molecules that were residing on the surface. If a molecule bounced off the surface, its interactions with the rest of the molecules on the surface were switched off if the vertical distance of its centre of mass from the substrate exceeded 7 Å, and were then switched back on when it dropped below this value. Figure 1(b) shows the snapshot of the system when three molecules had soft-landed on the surface, and figure 1(c) shows the final state when 12 out of the 14 molecules had been adsorbed and equilibrated with the substrate; the other two molecules, undergoing periodic boundary conditions, are not shown here. Figure 1(d) shows the top view of figure 1(c). The equilibrium configuration of the 12 molecules on the surface was reached after a significant period of 153 picoseconds from the start of the deposition process. The system was again equilibrated for a further eight picoseconds during which the molecules displayed some surface diffusion before

reaching the final alignment shown in figure 1(c), which corresponds to the configuration obtained after 161 picoseconds. In figure 1(c) the gaps between the centres of mass of the adsorbed molecules and the top basal plane are in the range of 6.47 Å to 6.57 Å. This is very close to the value 6.52 Å obtained by Rey *et al* [25] and also by Gravil *et al* [26]. In figure 1(d), the centre-to-centre inter-molecular separations are on average 9.9 Å. The alignment of the molecules in this figure strongly resembles the alignment reported in figure 2 for the STM-based experiment under UHV conditions [21], and also that obtained computationally by Rey *et al* [25].

As was discussed above, in a recent experiment [22] it was observed that the C_{60} islands predominantly nucleated near the step edges of the substrate. This observation was based on a scan of a substrate of area $2.2 \times 3.0\ \mu m^2$. In contrast, the sizes of our substrate basal planes were, at most, not more than about 25 nm^2. This implies that our substrate terraces corresponded to surface areas very close to the step edges of the substrate used in the experiment [22]. Hence, considering the size of our substrate, we can state from our figure 1(d) that the C_{60} film in our simulation also nucleated fairly close to the step edge. A larger-size system, which would have demanded a far longer period of simulation, would have improved the statistics with respect to the influence of the step edges and the importance of terrace sizes for the film growth. Moreover, it would have allowed us to reveal the mechanism of formation of the second and higher layers of the C_{60} film.

3. Computation of the STM-like images

According to the STM-based experiment of Yu *et al* [23], extra structures, in the form of 'bumps' and 'ridges', were observed on individual adsorbed C_{60} molecules. These features, reported to have dimensions of 1.6 Å to 2.5 Å, varied from one molecule to the next. It was stated that if they did indeed belong to the C_{60} molecules, then there must have been electronic states in close proximity to the Fermi energy, E_f, contributing to the STM tunnelling current. However, since a recent calculation [36] had shown that neither the energy of the lowest unoccupied molecular orbital (LUMO) nor that of the highest occupied molecular orbital (HOMO) of C_{60} is close enough to E_f to contribute to the tunnelling current, the suggestion was advanced that one probable cause could be the graphite substrate acting as a source of induced perturbations in the electronic states of the adsorbed molecules and providing the states necessary for imaging the purported 'ridges' and 'bumps'. On the other hand, in order to obtain high atomic resolutions, the experiment had to be performed with a very small tip-to-sample distance (about 3.3 Å) where the dominant contribution to the tunnelling current originates from the d_{z^2} state of the d-band metal, W, used as the tip. It was, therefore, further suggested that tip-induced states could also constitute another probable cause of these features. Owing to the complexity of this problem, in this paper we examine one of these probable causes, namely whether these features could have originated from the states induced by the W tip under the prevailing experimental conditions, i.e. a small tip-to-sample distance and a constant-current mode of imaging. The probable role of the substrate will be examined in another publication.

3.1. The tunnelling current

Since the STM operates under non-equilibrium conditions, the non-equilibrium Green function method of Keldysh [37] offers a very suitable basis for computing the tunnelling current and analysing the results obtained from a STM-based experiment. The computations of the STM-like images presented in this section were, therefore, based on this method, whose details are described elsewhere [38]. The method, as adapted to the STM theory [39], allows us to

consider the electron tunnelling between a tip and a sample as a superposition of the coherent tunnelling through different orbitals of the tip and the sample. As the method is not based on any perturbation expansion, unlike the Tersoff–Hamann approach [40], it is quite accurate at very small tip-to-sample distances.

In the application of this method to a STM problem, we start with the complete Hamiltonian of the tip–sample system which can be written as a combination of three terms corresponding to the tip ($\hat{H}_T$), the sample ($\hat{H}_S$) and the interaction between them ($\hat{H}_I$):

$$\hat{H} = \hat{H}_T + \hat{H}_S + \hat{H}_I. \tag{7}$$

The interaction term can be represented by a superposition of the hopping processes between the orbitals of the tip and those of the sample, i.e. we can express the $\hat{H}_I$-term as

$$\hat{H}_I = \sum_{\alpha j} [\hat{T}_{TS}(\alpha j)\hat{c}_T^{\dagger}(\alpha)\hat{c}_S(j) + \hat{T}_{ST}(j\alpha)\hat{c}_S^{\dagger}(j)\hat{c}_T(\alpha)] \tag{8}$$

where $\hat{T}_{TS}$ denotes the hopping matrix for hopping between the orbitals of the tip and the sample, and $\hat{c}_T^{\dagger}$, $\hat{c}_T$, $\hat{c}_S^{\dagger}$, $\hat{c}_S$ are the creation and annihilation vector operators associated with the orbitals of the tip (T) and the sample (S). The sum runs over all the orbitals in the tip (α) and the sample (j). In a steady state (determined by the applied voltage) the tunnelling current between the tip and the sample takes on the form [41]

$$J = \left(\frac{\mathrm{i}e}{\hbar}\right) \sum_{\alpha j} [\hat{T}_{TS}(\alpha j)\langle \hat{c}_T^{\dagger}(\alpha)\hat{c}_S(j)\rangle - \hat{T}_{ST}(j\alpha)\langle \hat{c}_S^{\dagger}(j)\hat{c}_T(\alpha)\rangle]. \tag{9}$$

Keldysh's theory then allows us to reformulate this expression in terms of Green functions [38]:

$$J = \left(\frac{4\pi e}{\hbar}\right) \int_{-\infty}^{+\infty} \mathrm{Tr}[\hat{T}_{TS}\hat{\delta}_{SS}(\omega)\hat{D}_{SS}^{R}(\omega)\hat{T}_{ST}\hat{\delta}_{TT}(\omega)\hat{D}_{TT}^{A}(\omega)][f_T(\omega) - f_S(\omega)]\,\mathrm{d}\omega \tag{10}$$

where

$$\begin{aligned} \hat{D}_{SS}^{R}(\omega) &= [\hat{I} - \hat{T}_{ST}\hat{g}_{TT}^{R}(\omega)\hat{T}_{TS}\hat{g}_{SS}^{R}(\omega)]^{-1} \\ \hat{D}_{TT}^{A}(\omega) &= [\hat{I} - \hat{T}_{TS}\hat{g}_{SS}^{A}(\omega)\hat{T}_{ST}\hat{g}_{TT}^{A}(\omega)]^{-1} \end{aligned} \tag{11}$$

where ($\hat{g}_{TT}^{R}$, $\hat{g}_{TT}^{A}$) and ($\hat{g}_{SS}^{R}$, $\hat{g}_{SS}^{A}$) are respectively the retarded and advanced Green functions of the tip and the sample, $\hat{\delta}_{TT}$ and $\hat{\delta}_{SS}$ are the corresponding densities of states and $f_{T,S}(\omega)$ are the Fermi–Dirac distributions for the tip and the sample respectively. The Green functions and the density-of-states matrices that appear in (10) correspond to the case when the tip and the sample are uncoupled (i.e. when $\hat{T}_{TS} = 0$). To calculate J we also have to compute the matrix $\hat{T}_{TS}$ with hoppings between the orbitals of the tip and the sample. It has been shown [42] that these hopping interactions can be calculated from the Bardeen tunnelling current between atomic orbitals ψ_i and ψ_j according to

$$T_{i,j} = -(1/2) \int_{\sigma_{ij}} (\psi_i \nabla\psi_j - \psi_j \nabla\psi_i)\,\mathrm{d}\boldsymbol{s} \tag{12}$$

and this method was employed in our present calculations.

3.2. Computation of C_{60}–graphite STM-like images

To examine the results of the experiment [23], we employed a tungsten tip. The tip was constructed using the cluster Bethe lattice method [43] where the top part of the tip was represented by a cluster of a few atoms and the influence of the rest of the tip's structure was

simulated by a Bethe lattice coupled to this cluster. We assumed that this top section of the tip was in the form of a pyramid with a single atom at its apex and four atoms at its base.

The calculations of the density of states and Green function matrices, necessary for the computation of J, were based on the linear combination of atomic orbitals (LCAO) Hamiltonian with the parameters taken from [44], and were performed self-consistently by imposing a local charge neutrality at each atom of the cluster. The LCAO approach was also used for the description of the C_{60} molecules and the graphite substrate. In our present computations we were concerned with investigating whether the observed intra-molecular features, if real, were due to tip-induced states caused by the experimental conditions. We therefore did not consider the interactions between the substrate and the C_{60} molecules, and also ignored the inter-molecular interactions. These assumptions implied that in this study the electronic structure of each C_{60} was essentially the same as that of an isolated C_{60}, i.e. having an energy gap of 2 eV between its HOMO and LUMO states. The positions and orientations of the molecules with respect to each other and with respect to the graphite substrate were those that were obtained from the MD simulation shown in figure 1(d).

To simulate the experimental imaging conditions as closely as possible, we performed our STM-like computations in a constant-current mode, keeping the tip-to-sample separation, i.e. the distance from the apex of the tip to the top of the adsorbed molecule, around 3.3 Å, exactly as in the experiment. A previous theoretical prediction [45] had shown that tunnelling through the d states of the apex atom in the tip could increase the resolution and the corrugation of the STM images in comparison with the results obtained from the s state of the tip. The smallness of the tip-to-sample distance (3.3 Å) in the experiment must have considerably increased the contribution of the d_{z^2} orbital of the apex tip atom to the tunnelling current and must have therefore been responsible for the high resolutions achieved in the STM images. It should, however, be pointed out that since the experiment was performed in air, and not under UHV conditions, the contamination of the tip by impurities was a real possibility, and in that case the role of the d_{z^2} state of the W tip for obtaining high-resolution images would not be so clear cut. Furthermore, it is also known that [38, 46] with a small tip-to-sample separation the topography of the STM images may show artificial features which are not consistent with the real charge distributions in the sample. The appearance of such features may be caused by the tunnelling through those orbitals of the apex atom in the tip that are oriented parallel to the $(x–y)$ plane, assuming that the z-axis represents the direction perpendicular to the substrate surface. Under some conditions, i.e. a small tip-to-sample distance and a sufficiently high density of states, the tunnelling through these orbitals can produce artificial features in the STM images of the surface structure, such as an inverted corrugation or the image of an adsorbed atom with a crater-like form [38, 46], neither of which correspond to the real charge distribution in the sample.

Our STM-like computations were performed on a single 'frozen' molecule extracted from the equilibrium system of the C_{60} molecules adsorbed on the graphite substrate in the MD simulation at room temperature and shown in figure 1(d). The justification for considering the position of the molecule as frozen during this computation, while C_{60} is relatively weakly bound to the substrate at room temperature, rests mainly on the experimental results where in figure 2 for the experiment in [23], STM images obtained in air and collected at 20-minute intervals showed a high degree of reproducibility i.e. during the scan the positions and orientations of particular molecules were fairly constant. It should, however, be added that there is always the possibility of the tip influencing the adsorption state of scanned atoms and molecules. Indeed, as has been shown theoretically [47] even in an imaging mode the STM tip could induce a *residual motion* to an atom (Xe) adsorbed on a surface (Cu(110)). However, it was shown that [47] this residual motion had a small influence on the STM image of the adsorbate where

the protrusion of the Xe adatom had a halfwidth about 0.6 Å larger than the corresponding image obtained from static calculations (figure 2 of [47]). If a similar influence of the W tip on the adsorbed C_{60} molecule were to be included in the calculations, then the STM-like image obtained would be different in some details compared with that obtained from a static molecule; we expect the width of the image to be increased and some changes in the positioning and size of intra-molecular features, especially near the edges of the image, to appear. The changes in the image of the topmost central part of the molecule would, probably, not be significant. In the experimental results [23], the diameter of the C_{60} ball was obtained to be 13 Å and the inter-molecular distance was 14 Å. Other predictions stated in [23] suggested that for a close-packed system the image of each ball had to be about 11 Å in diameter, while the image of an isolated C_{60} molecule obtained by means of a really sharp tip with a d_{z^2} state would have a diameter of 17 Å. This latter result agrees well with our result of 16.9 Å for the diameter. The fact that the inter-molecular distance in the experiment was found to be greater than that corresponding to a close-packed system of molecules suggests that the diameters of the molecules were in the range 11 Å to 17 Å. From this, it is not possible to infer the presence of a tip-imparted residual motion of individual C_{60} molecules, as was the case with the Xe atom [47]. However, we can speculate that this tip-imparted motion, if it did take place in the experiment, did not significantly change the characteristic features of the LUMO and the HUMO images in the topmost part of the scanned molecule, and it could certainly not have been the source of the extra features purported to have been observed for the molecules.

Figures 2 and 3 show respectively the HOMO- and the LUMO-like images of the single adsorbed C_{60} molecule obtained from our computations; the position and orientation of this molecule were obtained from our MD results shown in figure 1(d). In both the HOMO and the LUMO images, the positions of the carbon atoms in the upper part of the molecule are marked. We can see that a six-membered ring is approximately parallel to the surface. This is in line with the theoretical calculation [26] where it was found that such a configuration corresponded to the most stable orientation of the C_{60} molecule on the graphite surface irrespective of the position within the surface unit cell. Figure 4 shows an example of the scanline for the tip passing over the adsorbed molecule in our computations. It was extracted from the HOMO-like image shown in figure 2.

Detailed analysis of the contributions to the tunnelling current from different orbitals clearly showed that the central regions in both figures 2 and 3 were mainly built up from the tunnelling through the d_{z^2} orbital of the tungsten tip's apex atom; this contribution constituted around 60% of the total tunnelling current. The perpendicular orientation of the d_{z^2} orbital, with respect to the $(x–y)$ plane, enabled tunnelling from the part of the sample directly located below the tip and therefore we believe that the scanning did correctly reproduce the charge distribution of the C_{60} molecule. In fact, in both figures 2 and 3 the topographies of the images correspond very well to the charge distribution of the HOMO and the LUMO states of an isolated C_{60} molecule. Our HOMO-like image confirms that the HOMO states were mainly localized on the hexagonal rings. The image also shows the characteristic holes in the centres of the topmost hexagons representing the typical element of the charge distribution of the HOMO states. This topography is in agreement with the charge distribution of the HOMO states obtained in another theoretical study [48] and with the experimental results for scanning C_{60} molecules adsorbed on the Cu(111) surface [48] as well as those weakly physisorbed on the Si(100) surface [49]. In both of these latter cases the influence of the substrate on the electronic properties of the adsorbed C_{60} was found to be rather weak and therefore the STM images had topographies very similar to that of an isolated C_{60} molecule, as in our computations.

The LUMO states of a free C_{60} are located along the single C–C bonds, which make the maxima in the LUMO density of states appear at the pentagonal rings. This fact is clearly

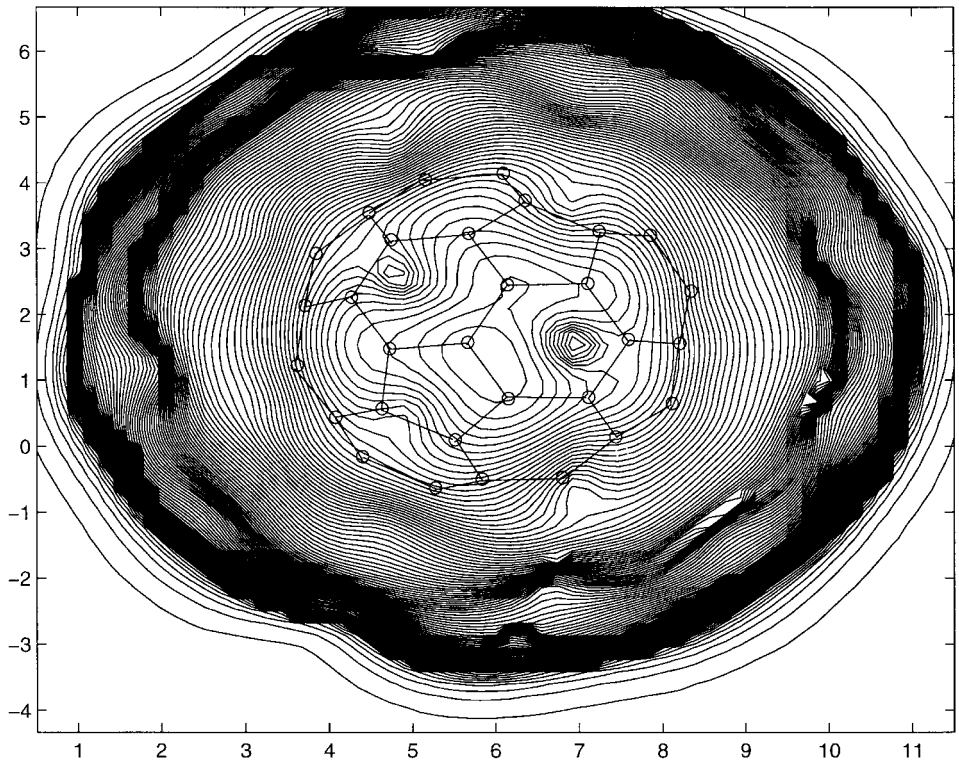

Figure 2. The computed STM-like image of the HOMO band for a C_{60} molecule extracted from figure 1(d). The positions of the atoms and the bonds of the top part of the molecule are indicated. The scales are in the units of the nearest-neighbour distance between the carbon atoms in an ideal C_{60} molecule, i.e. 1.41 Å. The horizontal and vertical axes refer to the (x, y) coordinates of the tip along the surface.

borne out by our numerical results. Figure 3 shows that the dominating features in the central part of our LUMO-like image are located at the three topmost pentagonal rings. Our computed topography compares with the results of calculations of the density of states of the LUMO states of the C_{60} molecule as well as with the STM-based LUMO-like images of the C_{60} molecules adsorbed on the Cu(111) surface, where it can be observed that the influence of the Cu substrate did not change the localization properties of the LUMO and the HOMO states of the C_{60} [48].

The size of the C_{60} molecule in the HOMO- and the LUMO-like images obtained from our computations was larger than its van der Waals diameter, and this is due to the tip–sample convolution effect which is also known experimentally [49]. The tunnelling resistance obtained in our computations was 12 MΩ. This value compares very well with those obtained in the experiment [23] (10 MΩ to 20 MΩ), the examination of whose results was the aim of our computations. This value was, however, much smaller than those obtained in the UHV-based STM experiments, such as [21], where it was found to be about 11 GΩ. This discrepancy must be attributed to the smallness of the tip-to-sample distance employed both in the experiment [23] and our computations where our aim was to test the validity of the claim that the d_{z^2} state of the W tip might have been responsible for the emergence of the purported extra features.

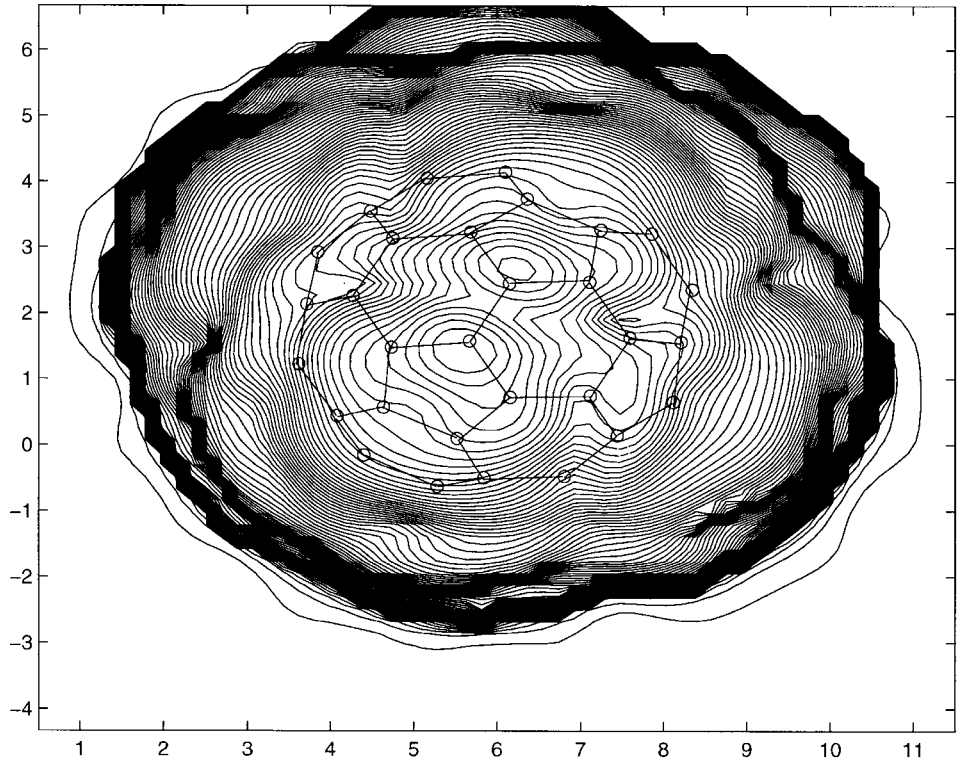

Figure 3. The computed STM-like image of the LUMO band for a C_{60} molecule extracted from figure 1(d). The positions of the atoms and the bonds of the top part of the molecule are indicated. The scales and the axes are the same as those in figure 2.

Summarizing the results of our STM-like computations, we can state that our accurate results on the charge distribution of the C_{60} molecule adsorbed on the graphite substrate did not show the presence of any extra states, and this would rule out the possibility that the reported intra-molecular features observed in the experiment [23] originated from the tip-induced states during the scanning process. The structure of these observed features is very different from the topographies of the LUMO- or the HOMO-like images of a free C_{60} or a C_{60} physisorbed on the Si(100) or on the Cu(111) surface. The origins of these ridges and bumps, if they are indeed real structures and not some experimental anomalies connected with the presence of impurities on the surface or the contamination of the tip by the C_{60} molecules themselves, must be looked for elsewhere, such as in the influence of the graphite substrate.

4. Conclusions

Our MD simulation results show that the combination of several widely different inter-atomic potentials to model the energetics and dynamics of carbon clusters together with the use of a complicated technique of soft-landing and adsorption of the C_{60} molecules were capable of reproducing the alignments of these molecules on a graphite substrate obtained both in a previous theoretical work and also observed experimentally in an STM-based experiment performed under UHV conditions at room temperature. The calculations of the STM-like

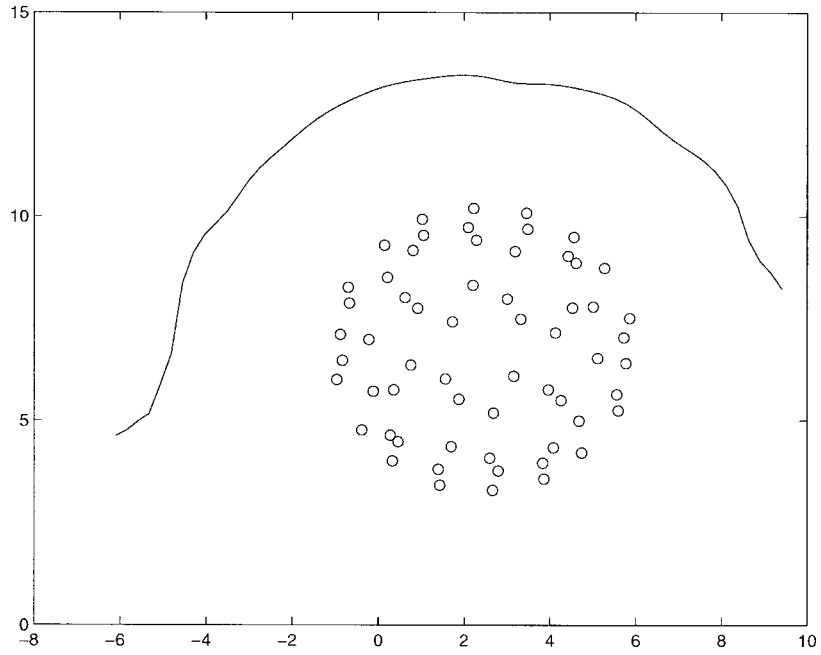

Figure 4. The scanline of the W tip passing over the adsorbed molecule. The line was extracted from the HOMO-like image in figure 2. The (x, y) coordinates are in Å. The $y = 0$ line corresponds to the position of the substrate.

images of one of the adsorbed molecules showed that the major contribution to the tunnelling current came from the d_{z^2} orbital of the W tip atom. This was a consequence of the electronic structure of the tip and the localization properties of the d_{z^2} orbital of tungsten. The topography of our STM-like images corresponded fairly accurately to the HOMO and the LUMO states of a free molecule. This confirmed that the experimental conditions that we used in our computations, i.e. a very small tip-to-sample separation, a constant-current mode of imaging and a tungsten tip, would not have been likely to cause the extra features in the charge states of the molecules. It seems likely, and this will be examined in a forthcoming publication, that if these features were indeed real, then their probable cause was the p_z state of the graphite substrate.

Acknowledgment

The authors are grateful to the British Council for financial support under the British–Polish Joint Research Collaboration Programme via Grant No WAR/992/130

References

[1] Tada T and Kanayama T 1996 *Japan J. Appl. Phys.* **35** L63
[2] Robinson A P G, Palmer R E, Tada T, Kanayama T and Preece J A 1998 *Appl. Phys. Lett.* **72** 1302
[3] Wang Xiang-Dong, Hashizume T and Sakurai T 1992 *Mod. Phys. Lett.* B **8** 1597
[4] Altman E I and Colton R J 1993 *Surf. Sci.* **295** 13
[5] Gimzewski J K, Modesti S, David T and Schlittler R R 1994 *J. Vac. Sci. Technol.* B **12** 1942
[6] Gimzewski J K, Modesti S and Schlittler R R 1994 *Phys. Rev. Lett.* **72** 1036

[7] Motai K, Hashizume T, Shinohara H, Saito Y, Pickering H W, Nishina Y and Sakurai Y 1993 *Japan. J. Appl. Phys.* **32** L150
[8] Kuk Y, Kim D K, Suh Y D, Park K H, Noh H P, Oh J S and Kim S K 1993 *Phys. Rev. Lett.* **70** 1948
[9] Hashizume T, Wang X-D, Nishina Y, Shinohara H, Saito Y, Kuk Y and Sakurai T 1992 *Japan. J. Appl. Phys.* **31** L880
[10] Li Y Z, Chander M, Partin J C, Weaver J H, Chibante L P F and Smalley R E 1992 *Phys. Rev.* B **45** 13 837
[11] Gensterblum G, Pireaux J J, Thiry P A, Caudano R, Vigneron J P, Lambin Ph, Lucas A A and Krätschmer W 1991 *Phys. Rev. Lett.* **67** 2171
[12] Lucas A A, Gensterblum G, Pireaux J J, Thiry P A, Caudano R, Vigneron J P, Lambin Ph and Krätschmer W 1992 *Phys. Rev.* B **45** 13 694
[13] Rafii-Tabar H, Kamiyama H, Maruyama Y, Ohno K and Kawazoe Y 1994 *Mol. Simul.* **12** 271
[14] Lamb L D, Huffman D R, Workman R K, Howells S, Chen T, Sarid D and Ziolo F 1992 *Science* **255** 1413
[15] Wilson R J, Meijer G, Bethune D S, Johnson R D, Chambis D D, de Vries M S, Hunziker H E and Wendt H R 1990 *Nature* **348** 621
[16] Li Y Z, Partin J C, Chander M, Weaver J H, Chibante L P F and Smalley R E 1991 *Science* **252** 547
[17] Li Y Z, Partin J C, Chander M, Weaver J H, Chibante L P F and Smalley R E 1991 *Science* **253** 429
[18] Hunt M R C and Palmer R E 1996 *Surf. Rev. Lett.* **3** 937
[19] Luo M F, Li Z Y and Alison W 1998 *Surf. Sci.* **402–404** 437
[20] Suto S, Kasuya A, Hu C-W, Wawro A, Goto T and Nishina Y 1996 *Surf. Rev. Lett.* **3** 927
[21] Suto S, Kasuya A, Hu C-W, Wawro A, Goto T and Nishina Y 1996 *Thin Solid Films* **281+282** 602
[22] Kenny D J and Palmer R E 2000 *Surf. Sci.* **447** 126
[23] Yu H, Yan J, Li Y, Yang W S, Gu Z and Wu Y 1993 *Surf. Sci.* **286** 116
[24] Ruoff R S and Hickman A P 1993 *J. Phys. Chem.* **97** 2494
[25] Rey C, Garcia-Rodeja J, Gallego L J and Alonso J A 1997 *Phys. Rev.* B **55** 7190
[26] Gravil P A, Devel M, Lambin Ph, Bouju X, Girard Ch and Lucas A A 1996 *Phys. Rev.* B **53** 1622
[27] Rafii-Tabar H 2000 *Phys. Rep.* **325/6** 239
[28] Dharamvir K and Jindal V K 1992 *Int. J. Mod. Phys.* B **6** 281
[29] Cheng A and Klein M L 1992 *Phys. Rev.* B **45** 1889
[30] Brenner D W 1990 *Phys. Rev.* B **42** 9458
[31] Brenner D W, Sinnott S B and Harrison J A 1997 private communication
[32] dwb@ripley.mte.ncsu.edu.
[33] Allen M P and Tildesley D J 1987 *Computer Simulation of Liquids* (Oxford: Clarendon)
[34] Nosé S 1984 *J. Chem. Phys.* **81** 511
[35] Hoover W G 1985 *Phys. Rev.* A **31** 1695
[36] Haddon R C, Burs L E and Raghavachari K 1986 *Chem. Phys. Lett.* **125** 459
[37] Keldysh L V 1964 *Zh. Eksp. Teor.Phys.* **47** 1515 (Engl. Transl. 1965 *Sov. Phys.–JETP* **20** 1018)
[38] Mingo N, Jurczyszyn L, Garcia-Vidal F J, Saiz-Pardo R, de Andres P L, Flores F, Wu S Y and More W 1996 *Phys. Rev.* B **54** 2225
[39] Ferrer J, Martin-Rodero A and Flores F 1988 *Phys. Rev.* B **38** 10 113
[40] Tersoff J and Hamann D R 1985 *Phys. Rev.* B **31** 805
[41] Caroli C, Combescot R, Nozières P and Saint-James D 1971 *J. Phys. C: Solid State Phys.* **4** 916
[42] Flores F, Martin-Rodero A, Goldberg E C and Duran J C 1988 *Nuovo Cimento* D **10** 303
[43] Martin-Moreno L and Verges J A 1990 *Phys. Rev.* B **42** 7193
[44] Papaconstantopoulos D A 1986 *Handbook of the Band Structure of Elemental Solids* (New York: Plenum)
[45] Chen C J 1990 *Phys. Rev. Lett.* **65** 448
[46] Flores F, de Andres P L, Garcia-Vidal F J, Jurczyszyn L, Mingo N and Perez R 1995 *Prog. Surf. Sci.* **48** 27
[47] Bouju X, Joachim C and Girard Ch 1999 *Phys. Rev.* B **59** R7845
[48] Hashizume T, Motai K, Wang X-D, Shinohara H, Saito Y, Maruyama Y, Ohno K Kawazoe Y, Nishina Y, Pickering H W, Kuk Y and Sakurai T 1993 *Phys. Rev. Lett.* **71** 2959
[49] Yao X, Ruskell T G, Workman R K, Sarid D and Chen D 1996 *Surf. Sci.* **367** L85